END-TO-END SIMULATION AND ANALYSIS FRAMEWORK FOR EFFICIENT SEISMIC RETROFITTING OF WATER SYSTEMS

J. Wu[1], J. Baker[2]

[1] *Ph. D. Candidate, Stanford University, jwu11@stanford.edu*
[2] *Associate Professor, Stanford University, bakerjw@stanford.edu*

Abstract

Maintaining the functionality, productivity, and safety of communities necessitates the seismic reliability of lifeline infrastructure networks. However, assessing the reliability of an infrastructure network is a nontrivial task due to the variability of ground motion and the complexity of the response of the network resulting from that ground motion. Even more challenging is the task of identifying retrofit schemes that effectively and efficiently bolster the reliability of the network. Previous works have studied hazard identification, network reliability estimation, and network retrofitting, though somewhat independently. This paper extends and unifies previous work on these topics by establishing an end-to-end simulation and analysis framework that encompasses ground motion simulation, network component fragility, network modeling, and retrofit prioritization. By utilizing a full probabilistic description of the seismic hazard and integrating earthquake occurrence rates into the retrofit evaluation scheme, this framework not only identifies critical network components, but those critical components that are also likely to be damaged. A case study of the Auxiliary Water Supply System of San Francisco is used to demonstrate the procedure described in the proposed framework. This paper shows that this framework contributes retrofitting heuristics that inform existing methods of pipe retrofitting prioritization such that more effective retrofits are obtained.

Keywords: Lifeline networks, Infrastructure network retrofitting, Probabilistic Seismic Hazard Analysis

1. Introduction

The functionality of lifeline networks is critical for the functionality, productivity, and safety of modern society—basic services such as power, water, telecommunications, and roads allow businesses to operate, emergency services to be responsive, and households to live their way of life. Natural hazards impede these services by damaging or destroying network components, disrupting the normal operation of our communities.

Investments in infrastructure network reliability would aid in mitigating both physical and economic damage and expedite recovery from future events, such as earthquakes. A seismically reliable network minimizes damage and hastens the restoration of its components, as well as facilitates the recovery of other infrastructure networks, as [1] report significant operational interdependencies between networks from analyzing post-earthquake restoration curves. Quick restoration of infrastructure networks minimizes indirect losses in the commercial sector due to business interruption: resilient water delivery and electrical power networks help minimize the financial losses that would accrue daily due to facility shutdown; business activities involving the transport of goods may resume sooner with a reliable transportation network. Additionally, post disaster network operability may also be critical in maintaining community safety after the primary event. Engineers must be able to access structures to evaluate their safety and integrity, while essential healthcare facilities (e.g. hospitals) rely on the functionality of power, water, and wastewater systems to maintain their services [2, 3]. Furthermore, fires following earthquakes necessitate the survival of the water supply system to combat these fires and minimize conflagration [4].

In preparation for future earthquakes, cities may opt to strengthen the various components of the water system to improve the seismic reliability of the network. However, assessing the reliability of an infrastructure network is a nontrivial task due to the variability of ground motion and the complexity of the response of the network resulting from that ground motion. Even more challenging is the task of identifying retrofit schemes that effectively and efficiently bolster the reliability of the network. To best accomplish this arduous task, the following components must be understood and integrated: hazard identification, network performance assessment/reliability estimation, and network retrofitting. Previous works have studied these topics though somewhat independently.

Many methods have been developed for the risk and reliability assessment of lifeline infrastructure networks, such as the work by [5, 6]. While these papers provide significant insight as to the estimation and prediction of the performance of networks subjected to natural hazards, none of them proceeded to address the question of what we should do to improve network performance. Similarly, there have been many methods developed for determining the most efficient schemes for retrofitting lifeline networks, such as the work by [7-10]. Very few of the metrics explored in these papers integrate the probability of the failure of the network component into the evaluation of component importance. Additionally, all of these metrics by definition evaluates component importance independent of each other, and fails to capture the effects of joint failures, which is a significant drawback due to the correlated nature of the ground motion (and hence, the correlated nature of component damage).

Emerging research in the topic of lifeline network seismic resilience has endorsed the integration of seismic hazard into retrofit planning. [11] prescribe hazard identification and component fragilities to water agencies as essential aspects of schemes for retrofitting to improve community resilience. [12] propose a simulation based seismic risk assessment methodology for gas distribution networks and demonstrates a deaggregation approach that may aid in determining effective retrofits. With regards to bridge retrofitting, the United States Federal Highway Administration provides guidelines for retrofit prioritization that considers both bridge vulnerability and the consequence of bridge failure [13]; however, [14] notes that the proposed guidelines involve analyzing bridges independently and fail to capture correlated bridge failures and the increased severity of network disruption from multiple bridge failures. They explore a bridge rank measure based on expected replacement cost given the seismic hazard, as well as the traffic volume based importance measure, and propose a composite measure that encompasses the aforementioned two importance measures. This composite measure ranks bridges according to their participation in damage maps resulting in high loss in network performance, weighted by the occurrence rate of those damage maps. These damage maps are simulated using realistic ground

motion maps, and thus reflect potential future damage scenarios while capturing the impact of multiple bridge failures.

This paper extends and unifies previous work on these topics by establishing an end-to-end simulation and analysis framework that encompasses ground motion simulation, network component fragility, network modeling, and pipe retrofit prioritization. This framework allows the calculation of the Theoretical Pipe Participation Factor (TPPF), a metric that may be utilized as a retrofit heuristic and that is informed by seismic reliability analysis. This paper will show that TPPF informs existing pipe retrofitting methods to yield more effective retrofit schemes. Note that this work currently focuses on the retrofitting of pipelines; while water storage tanks and pumping stations are susceptible to damage from ground motion and may be candidates for retrofit, that is left for future work.

The remainder of this paper is organized as follows. Section 2 discusses how lifeline networks are modeled in this work, as well as introduces the case study network to demonstrate the proposed methodology. Section 3 describes the procedure for ground motion simulation used in this paper. Section 4 describes the procedure for modeling and estimating network performance used in this paper. Section 5 discusses the formulation of retrofitting heuristics and investigates their effectiveness. Section 6 summarizes the significance of the findings in this paper, as well as briefly discusses opportunities for future work.

2. Description of Water Supply Networks and Case Study Network

This section gives a brief description of how infrastructure networks are to be modeled, as well as the case study network used to demonstrate the proposed methodology.

Here, lifeline networks are modeled as a set of nodes and a set of links. Nodes represent points in the network where resources are introduced (source nodes), consumed (distribution nodes), or modified, while links are pathways through which resources travel between nodes. This paper utilizes EPANET, software developed by the EPA that models the hydraulic behavior of water distribution networks [15]. Within EPANET, pipe junctions, reservoirs, and tanks are modeled as nodes in the network, while pipes, valves, and pumps are modeled as links.

To demonstrate the proposed framework, this paper studies the Auxiliary Water Supply System (AWSS) of San Francisco, shown in Fig. 1. The AWSS is composed of approximately 6200 nodes, including 2 tanks and 1 reservoir, and 6300 pipe segments spanning about 205 kilometers. Pipe material is assumed to be of cast iron if the pipe segment was laid prior to 1970 according to records, and of ductile iron if the pipe segment was laid after 1970. Approximately 172 kilometers of pipeline are assumed to be of cast iron, and the remaining 33 kilometers of pipeline are assumed to be of ductile iron. Water demands in this network reflect fire-fighting demands due to a 7.9 M_W North San Andreas earthquake. The authors acknowledge that water demands should change with the particular earthquake scenarios this network is subjected to, but opt to fix demands to reflect the above described scenario for simplicity, as fire-fighting demand simulation is outside of the scope of this work.
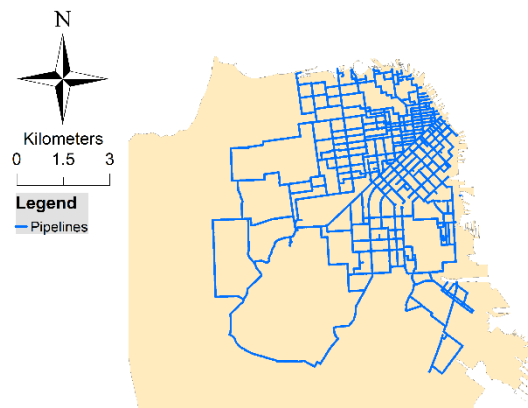
Fig. 1 - Pipelines of the Auxiliary Water Supply System in San Francisco

3. Generation of Ground Motion Maps

This section summarizes the procedure for generation of ground motion maps for the assessment of network seismic reliability. This procedure uses probabilistic risk assessment in order to track uncertainties and consider a range of potential future earthquake scenarios; the value of this choice relative to a scenario-based risk assessment is discussed elsewhere [16–18].

Step 1: Generate all feasible earthquake scenarios for the area of interest. This study utilizes OpenSHA [19], an open source Java-based platform for conducting seismic hazard analysis, to enumerate all pertinent earthquake scenarios in the area of interest. For San Francisco, the OpenSHA application generated 2,430 scenarios using the Uniform California Earthquake Forecast 2 model (UCERF2) developed by the Working Group on California Earthquake Probabilities (WGCEP) [20]. These scenarios consider all ruptures within 200 km of the area of interest, with various increments of earthquake magnitudes, rupture lengths, and rupture locations.

Step 2: Calculate the median and dispersion of the intensity measures (IMs) at all points of interest using ground motion prediction equations (GMPEs) for each scenario generated in Step 1. In this study, the Boore and Atkinson (2008) GMPE is used to calculate the median and dispersion of the peak ground velocity (PGV) in the San Francisco area for the purpose of pipe fragility estimation later in this framework. The IMs are evaluated in a rectangular grid of regularly spaced sites in San Francisco, with 500-meter spacing between sites, and site to rupture distances are calculated using the rupture locations collected in Step 1. This study utilizes V_{s30} values estimated from boring data in San Francisco.

Step 3: Simulate a random field over the area of interest using the median and dispersion parameters from Step 2, considering spatial correlation between entries. Many previous works have highlighted the importance of spatial correlation when modeling losses due to earthquakes [16, 17, 21]. In this paper, the ground motion values at each site are simulated according to the equation below.

$$\ln \overline{Y}_{ij} + \phi_{ij}\varepsilon_{ij} + \tau_j\eta_j = \ln Y_{ij}$$

(1)

Where $\overline{Y}_{ij}$ is the median ground motion for the ith site in the jth scenario, ϕ_{ij} and τ_j are the within-event and between-event residuals, ε_{ij} and η_j are random variables sampled during simulation, and Y_{ij} is the resulting realization of ground motion. For each particular jth scenario, the variable η is sampled from a standard normal distribution, and the variables ε for each site are sampled from a multivariate Gaussian distribution with covariance terms reflecting the spatial correlation between sites. This paper simulates the correlated ε terms by assuming an exponential model for correlation between sites found in [22] using methods described in [23]. For each scenario from Step 1, 10 PGV maps are simulated, such as the map depicted in Fig. 2, yielding a collection of 24,300 ground motion maps.

N

Kilometers
0   1.75   3.5

Legend

PGV (cm/s)

■ < 30
■ 30 - 60
■ 60 - 90
■ 90 - 120
■ > 120
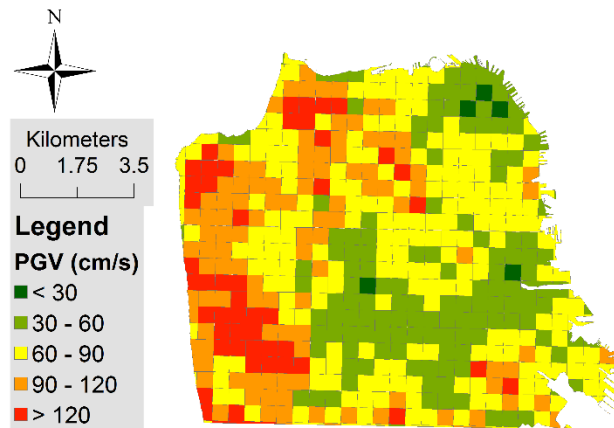
Fig. 2 – Simulated PGV map of an M_w 8.05 North San Andreas rupture at 500 m grid spacing.

Step 4: Optimize the ground motion map set. As using all ground motion maps for network reliability analysis would be prohibitively expensive, this step reduces the entire set of ground motion maps generated in the previous step, denoted as the baseline set, to a subset of representative maps, while maintaining the ground motion probabilities of the entire set. This paper utilizes the methods proposed in [24] which uses optimized reduction with convex relaxation. The hazard curves for the intensity measure of interest at various sites are calculated using the entire set of ground motion maps. Additionally, an easily obtained proxy measure is calculated for each ground motion map. This proxy measure provides additional assurance that the impact of the distribution of the ground motion (i.e. spatially correlation) will be preserved in the resulting network performance assessment using the resulting optimized subset. The method then attempts to find a subset composed of a target smaller number *k* maps with adjusted weights that minimizes the difference between the baseline and the subset in their ground motion hazard curves and annual exceedance curves of the proxy measure within the exceedance rates of interest.

Applying this method to this study, the set of ground motion maps is optimized using the PGV at 14 key sites distributed throughout San Francisco and the chosen proxy measure. The proxy measure used here is the mean number of leaks and breaks in the pipes throughout the network for a given ground motion map. This parameter assesses the spread of damage—and thus a sense of network performance—for each ground motion map. The mean number of leaks and breaks is calculated by translating ground motion values to pipe damage probabilities using the pipe fragility curves to be discussed in Section 4. The optimization procedure is performed on the collection of 24,300 ground motion maps from the previous step to find a representative subset composed of a target of 100 maps, yielding a finalized subset of 91 ground motion maps. Fig. 3 below depicts the hazard curves based on the entire set of ground motion maps, denoted "Baseline", and the hazard curves using the optimized subset of 91 ground motion maps, denoted "Subset", for one key site, as well as the proxy parameter of the mean number of leaks and breaks in the pipes of the network.
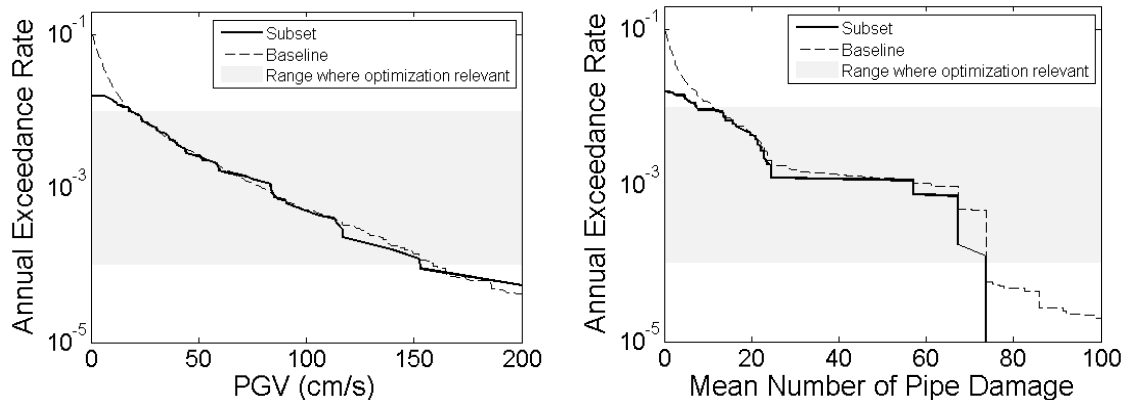
Fig. 3 – (Left) Hazard curve of entire ground motion set and optimized ground motion set for a key site. (Right) Annual exceedance curve of the proxy measure, the mean number of pipe leaks and breaks throughout the network, from the entire ground motion set and optimized ground motion set. The gray area signifies the exceedance rates of interest.

This optimized set of 91 PGV maps is passed on to the network models for seismic performance assessment, as described in the next section.

4. Estimating Performance of Networks subjected to Ground Motion

This section summarizes the steps used to subject infrastructure networks to the ground motions simulated in the previous section and estimate the resulting network performance.

Step 1. Translate ground motion intensity values to pipe damage probabilities. The ground motion experienced by each pipe as well as corresponding pipe material are used to calculate pipe break probabilities in

the form of repair rates using fragility curves provided in literature. To demonstrate this framework, this study opts to use fragility curves developed by Jeon and O'Rourke, who derive the curves from analyzing the correlation of pipe damage and PGV found in Los Angeles, California after the 1994 Northridge earthquake [25]. The fragility curves from Jeon and O'Rourke are believed to provide more precise estimates due to the similarity in composition between the water networks in Los Angeles and San Francisco [26]. The fragility curves for cast iron (CI) pipes and ductile iron (DI) pipes are described by the equations below:

$$R_{Rate} = \begin{cases} 0.0011 \times (PGV)^{1.12} \text{ (CI)} \\ 0.000083 \times (PGV)^{1.84} \text{ (DI)} \end{cases}$$

(2)

where R_{Rate} is the resulting repair rate and *PGV* is the maximum peak ground velocity.

While the procedure above describes the use of PGV for pipe fragility estimation, pipe fragility may incorporate other considerations, such as landslide and liquefaction susceptibility, as well as use other appropriate IM relations, such as PGD.

Step 2. Simulate pipe damage. Monte Carlo Simulation is used to generate the amount and location of damage within each pipe segment using the pipe repair rates calculated in the previous step as well as pipe lengths. Pipes may experience damage in the form of pipe breaks or pipe leaks. According to the American Lifelines Alliance, a pipe break is defined as "the complete separation of a pipeline, such that no flow will pass between the two adjacent sections of the broken pipe", whereas a pipe leak is defined as "a small leak in a pipeline, such that water will continue to flow through the pipeline, albeit at some loss of pressure and flow rate being delivered, with some flow being lost through the leak" [27]. Following Hazus recommendations, 20% of simulated damage are classified as pipe breaks, while the remaining 80% of simulated damage are classified as leaks [28]. For each of the 91 ground motion maps simulated in the previous section, 20 pipe damage simulations are performed following the parameters described above, yielding a total of 1,820 pipe damage sets.

Step 3. Run a network model to estimate network performance after subjecting the network to pipe damage simulated from the previous steps. There exist many different methods of modeling network performance with differing degrees of complexity. In the interest of maximizing the accuracy and realism of this study, this study utilizes GIRAFFE, software developed by Cornell University, to perform flow analyses of the case study water network [29]. Network topology, network attributes, such as pump power, valve status, tank and reservoir initial values, etc., and the set of pipe damage are first fed into GIRAFFE. GIRAFFE applies pipe damage by modifying the network topology such to mimic the hydraulic impacts of leaks and breaks. Using this modified network topology, GIRAFFE iteratively calls EPANET's hydraulic modeling engine. In each iteration, EPANET performs hydraulic flow simulation to obtain the set of pipe flow, nodal pressure, etc. that satisfies the governing flow equations. Then, GIRAFFE removes the nodes with negative pressure from the network, as well as pipes that have been disconnected from the network in the process. GIRAFFE then calls EPANET with this modified network. GIRAFFE continues iterating until there are no longer nodes with negative pressure in the network. Once this equilibrium is achieved, GIRAFFE outputs the final surviving network components with nodal pressures, pipe flow, etc., and serviceability of nodes—defined as the proportion of simulations that the distribution node is able to satisfy its demand—at various time increments after the application of pipe damage.

Pipe damage sets generated from the previous step are fed into GIRAFFE, and the resulting nodal serviceability, pipe flow, nodal pressure, etc. at time 0 (i.e. immediately after pipe damage is applied to the network) are tabulated for the calculation of network performance metrics described in the next step.

Step 4. Calculate network performance metrics and aggregating performance results into performance curves. Using the results output from GIRAFFE, we may assess the performance of the network subjected to the various ground motions simulated. This paper considers a number of global performance metrics—metrics that quantify the performance of the network overall.

The Nodal Unsatisfaction, *NU*, is a global network performance metric and defined here as the proportion of nodes that do not have their demands satisfied. The Nodal Unsatisfaction reflects the spatial extent of network disruption. Nodal Unsatisfaction may be calculated as follows.

$$NU = 1 - \frac{1}{|V|}\sum_{\forall i \in V} I\left[\hat{D}_i \geq D_i\right] \tag{3}$$

Where V is the set of nodes in the network, D_i is the water demand at node i, $\hat{D}_i$ is the amount of water available at node i up to a maximum amount of D_i, $I[\cdot]$ signifies the indicator function, and $|\cdot|$ signifies the cardinality of the set $\cdot$. Note that $I[\hat{D}_i \geq D_i]$ will take a value of 1 when the amount of water available at node i meets the water demand at node i, and 0 otherwise.

The Demand Unsatisfaction, DU, is a global network performance metric and defined here as the ratio of the total unsatisfied demand in the network to the total network demand. The Demand Unsatisfaction reflects the magnitude of network disruption. Demand Unsatisfaction may be calculated as follows.

$$DU = \frac{\sum_{\forall i \in V} D_i - \hat{D}_i}{\sum_{\forall i \in V} D_i} \quad \text{or} \quad DU = 1 - \frac{\sum_{\forall i \in V} \hat{D}_i}{\sum_{\forall i \in V} D_i} \tag{4}$$

These metrics estimate the performance of the network subjected to a particular ground motion map. After calculating the network performance for all simulated ground motion maps, annual exceedance rates of each performance metric may be calculated as follows.

$$\lambda(\hat{p}) = \sum_{j \in M} w_j I\left[P_j \geq \hat{p}\right] \tag{5}$$

Where $\lambda(\hat{p})$ is the annual exceedance rate of a specified network performance level $\hat{p}$, M is the set of all damage maps, w_j is the weight (i.e. the annual occurrence rate) of damage map j, P_j signifies the network performance resulting from damage map j, and $I[\cdot]$ signifies the indicator function. Note that $I[P_j \geq \hat{p}]$ will take a value of 1 when the network performance resulting from damage map j exceeds the specified network performance level, and 0 otherwise. Annual exceedance curves may be constructed after calculating the annual exceedance rates at various levels of the performance metric. Example plots of the annual exceedance curves of Nodal and Demand Unsatisfaction are presented in Fig. 4 below. These plots indicate, for example, that the annual exceedance probability of a Nodal Unsatisfaction level of 0.7 is approximately 0.005.
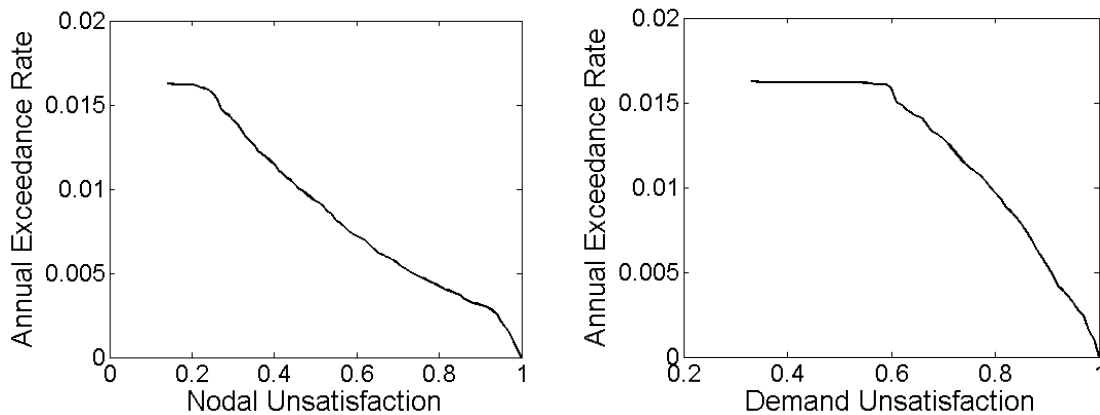
Fig. 4 – Example annual exceedance curves of nodal unsatisfaction (left) and demand unsatisfaction (right).

5. Developing Efficient Retrofit Schemes

This section discusses the methodology for developing efficient retrofit schemes pursued in this paper. As previously mentioned, various methods have been explored in the literature for the development of efficient retrofit schemes. Ideally, all possible schemes should be exhaustively explored such to discover the most optimal scheme. The knapsack approach proposed by [8], for example, would achieve such a result; however, such

exhaustive methods become prohibitively expensive for larger networks. Thus, this paper explores several heuristics that may inform us of near optimal solutions without having to perform an exhaustive search. Moreover, this paper pursues heuristics that consider both the network component vulnerability to seismic hazard and the contribution of the component to network performance.

Inspired by the composite importance measure developed by [24], this paper proposes the pipe importance heuristic Theoretical Pipe Participation Factor (TPPF). TPPF estimates the importance of a pipe segment by its participation in damage maps that yield high network disruption, computed as follows.

$$\text{TPPF}_{\text{component } i} = \frac{1}{L_i} \frac{1}{\sum_{j \in S_D} w_j} \sum_{j \in S_D} w_j P(x_{i,j} \geq x) \tag{6}$$

Where L_i is the length of the pipe segment i, w_j is the weighting factor of damage map j (here, taken to be the occurrence rate of damage map j), S_D is the set of damage maps that result in high network disruption, and $P(x_{i,j} \geq x)$ is the probability of pipe damage for pipe segment i in damage map j.

This formulation may be interpreted as finding the probability of a ground motion map contributing to high network disruption, and then finding the pipe segments that are likely to be damaged in those ground motion maps—thus those pipe segments with high TPPF should be those with high probability of damage in scenarios that contribute to high network disruption. The key feature here is the choice of only considering damage maps with high network disruption in S_D. If S_D included all damage maps rather than only the aforementioned subset, then Eq. (6) would simply capture pipe vulnerability, in the form of the annual probability of pipe damage, normalized by the pipe length. With a well-tuned criterion for S_D, TPPF reflects a sort of "smart" vulnerability estimate: the metric considers the vulnerability of pipes only in the scenarios that matter—that is, the scenarios that result in high network disruption.

One potential issue with the use of pipe damage probability in TPPF is the case where pipes are incidentally broken in damage maps in S_D. For example, pipe segments highly susceptible to damage may participate in many damage maps with high network disruption solely due to their high susceptibility to damage while not actually significantly contributing to network performance.

To complement TPPF, this paper also explores the heuristic Risk Achievement Worth (RAW), as defined by [9, 30], applied to water pipelines. RAW captures a pipe segment's singular contribution to the performance of the water network.

$$RAW_{component \ i} = \frac{F_S(Q_i = 1)}{F_S} \tag{7}$$

Where $F_S(Q_i = 1)$ is the network disruption when pipe segment i is damaged, and F_S is the network disruption with no pipe damage. Here, F_S may be regarded as the nodal unsatisfaction or the demand unsatisfaction. Unlike TPPF which finds pipe segment failures that are *correlated* with high network disruption, RAW by definition implies a degree of causality between pipe performance and network performance. However, [10] is cautious of its use, as it is rough: RAW does not integrate pipe vulnerability to seismic hazard, and only considers singular pipe damage, while typical seismic events yield multiple simultaneous failures which may contribute to higher network disruption than what is captured by RAW. These flaws are not present in TPPF, as TPPF extracts information from realistic damage maps that inherently captures pipe vulnerability and joint pipe failures. On the other hand, the issue of incidental pipe damage found in TPPF is not an issue in RAW, due to its implied causality. Thus, RAW serves as an interesting complement to TPPF.

The authors also propose a heuristic that combines the scores from TPPF and RAW. The objective in combining these two heuristics is to take advantage of the complementary nature of these heuristics and address the issues inherent in each of the heuristics individually. The Combined Measure is computed as follows.

$$Combined\ Measure_{component\ i} = 1 - \frac{\left(Rank_{TPPF,i} - 1\right) + \left(Rank_{RAW,i} - 1\right)}{2|E|} \tag{8}$$

Where $Rank_{TPPF,i}$ denotes the ranking of segment *i* in retrofit priority using the heuristic TPPF, $Rank_{RAW,i}$ denotes the ranking of segment *i* in retrofit priority using the heuristic RAW, *E* is the set of all pipe segments in the network, and |▪| denotes the cardinality of ▪.

To test the effectiveness of these retrofit heuristics, retrofit schemes are developed for the case study network AWSS described in section 2. Approximately 55 km of pipeline is selected for retrofit (approximately 25% of the network) using each of the discussed heuristics. Assuming retrofit costs are uniform per length of pipeline, each retrofit scheme has equivalent cost; then, the evaluation of the retrofit schemes in terms of cost/benefit ratio need only compare their relative benefits. For ease of calculation and to make the differences between the heuristics more explicit, the resulting "retrofits" cause the affected pipes to be invulnerable to damage. Retrofit schemes using TPPF, RAW, and the Combined Measure are depicted in Fig. 5 below.
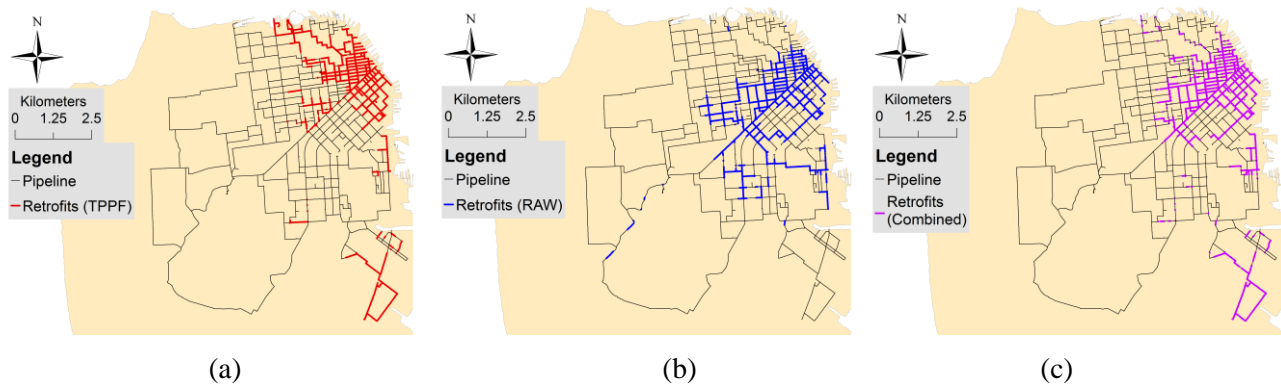
Fig. 5 – Retrofit schemes using (a) TPPF, (b) RAW, and (c) the Combined Measure.

The features of each heuristic can be seen in these resulting retrofit schemes. The retrofit scheme using TPPF depicted in Fig. 5 (a), focuses on pipes in the northeast part of the network without extending extensively west down Market Street, as well as some in the southeast. This selection of pipes reflects the objective of TPPF to determine those pipes that both contribute to network functionality and are likely to experience damage. The pipes chosen by TPPF have a mean annual probability of damage, normalized by pipe length, of 2.9×10^{-5}, compared to the mean annual probability of damage of pipes chosen by RAW being 2.7×10^{-5}. In the retrofit scheme using RAW depicted in Fig. 5 (b), we see the retrofit scheme focusing on pipe mains down Market Street, with excursions to the north and south of Market Street. The retrofits appear to be applied to core of the network, which are consistent with the objective of RAW to identify those pipe segments that significantly contribute to network functionality. Then in Fig. 5 (c), which depicts the retrofit scheme using the Combined Measure, this heuristic attempts to reconcile the differences between the retrofit schemes using RAW and TPPF. Retrofits are applied to the pipe mains down Market Street with limited excursions north and south of Market Street, slight extensions in the northeast as compared to RAW, and inclusion of the pipe repairs in the southeast as seen in TPPF. The mean annual probability of damage, normalized by pipe length, for pipes selected according to the Combined Measure is 2.8×10^{-5}.

The resulting network performance in the form of the annual exceedance of network disruption (nodal unsatisfaction and demand unsatisfaction) using these retrofit schemes are depicted in Fig. 6 below, with "TPPF", "RAW", and "Combined" denoting the use of the heuristics TPPF, RAW, and the Combined Measure, respectively. For comparison, these results are compared to a baseline reflecting the network performance with no retrofits, indicated by "Base" in the plots below, and a retrofit scheme using no heuristic—pipes are randomly selected for retrofits—indicated by "Random" in the plots below. The plots below are zoomed into the regions of interest.
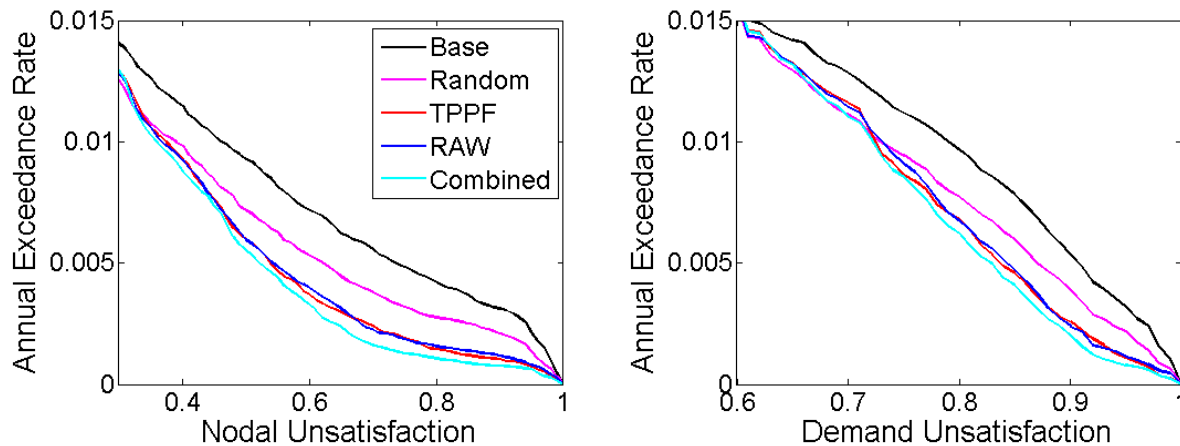
Fig. 6 – Annual exceedance curves of nodal unsatisfaction (left) and demand unsatisfaction (right) after retrofitting according to TPPF, RAW, and the Combined Measure TPPF+RAW, zoomed into the regions of interest.

From both plots in Fig. 6, the retrofits using the heuristics RAW, TPPF, and the Combine Measure perform significantly better than the random selection of retrofits. While RAW and TPPF individually appear to yield similar improvements to network performance, combining these heuristics via the Combined Measure yields further improvements to network performance. The improved performance of the Combined Measure suggests that a potential avenue for finding more appropriate pipe segments would be to inform RAW or TPPF with information from the other heuristic—that is, improvements to the heuristic RAW may be achieved by integrating information offered by TPPF, and vice versa. Additionally, the Combined Measure takes advantage of their features to address each other's limitations: incidentally broken pipes in TPPF are moderated by the information provided by RAW, while TPPF provides vulnerability information and group damage effects.

This section has demonstrated the value of TPPF in the development of retrofit schemes; and as the calculation of TPPF involves seismic hazard analysis, this section, by extension, has demonstrated the value of integrating seismic hazard analysis into retrofit planning.

6. Conclusions

This paper proposes an end-to-end simulation and analysis framework for estimating infrastructure network performance and prescribing efficient retrofits, which encompasses the topics of the selection and generation of ground motion maps, the modeling and estimation of network performance, and the determination of efficient retrofit schemes. This paper highlights various methodologies in each of these subjects, and discusses the preferred methods for this framework. In retrofit prioritization strategies, this work proposes the Theoretical Pipe Participation Factor retrofitting heuristic, as well as investigates an established retrofitting heuristic, the Risk Achievement Worth, for its ease of calculation and complementary nature to the Pipe Participation Factor. To address the individual limitations of these heuristics, these heuristics are combined using a formulation termed the Combined Measure. The choices of methodologies in each of the topics reflect the aim of this work to maximize the accuracy and realism of the network performance estimates to achieve retrofit schemes that are both efficient and applicable for implementation.

The proposed end-to-end framework is demonstrated using the case study network of the Auxiliary Water Supply System of San Francisco. The resulting retrofit schemes using the heuristics TPPF, RAW, and the Combined Measure are developed and compared. While TPPF and RAW appear to yield similar retrofit effectiveness, the Combined Measure further improves retrofit effectiveness, reflecting the ability of TPPF and RAW to inform each other to achieve a better measure of pipe importance. This demonstrates the value of TPPF as its integration into retrofit scheme development enables the achievement of higher network performance; in

turn, this demonstrates the value of the proposed end-to-end framework, as the integration of seismic hazard analysis of networks into retrofit planning enables the calculation of heuristics such as TPPF.

The procedure described above assumes that other components of the water network, such as water storage tanks and pumping stations, are invulnerable to damage. This assumption is made as this work is focused on the criticality and retrofitting of pipeline, and the evaluation of other network components is left for future work. However, the authors recognize that this assumption may impact the resulting retrofit scheme if there is a large disparity among these facilities in terms of reliability and pipelines serviced.

There are many avenues for future work to extend and refine the current analysis to further increase the fidelity of the results, such as the application to other lifeline infrastructure networks subjected to different hazards, the consideration of network interdependency, and the additional refinement of the retrofitting heuristics. Additionally, the retrofit heuristics may be modified to integrate social welfare (e.g. nodes servicing emergency services should have a higher priority) and economic considerations for better cost/benefit analysis (e.g. the cost of excavation and retrofits may not be uniform across the network). Furthermore, the retrofit heuristics may be adapted to consider other network components in tandem, such as the water storage tanks and pumping stations, and identify the most efficient combination of pipeline, tanks, and pumps to retrofit.

The primary objective of this work is to provide insight regarding efficient lifeline network retrofits to better mitigate damage from future seismic events and bolster community resilience. This task invariably requires the enumeration and management of the numerous sources of uncertainty inherent in this problem. The proposed framework discusses and prescribes methods to address these uncertainties in a structured manner, and, with continued refinement, may provide an avenue towards robust lifeline networks.

7. Acknowledgements

8. References

[1]   L. Dueñas-Osorio and A. Kwasinski, "Quantification of Lifeline System Interdependencies after the 27 February 2010 M $_w$ 8.8 Offshore Maule, Chile, Earthquake," *Earthquake Spectra*, vol. 28, no. S1, pp. S581–S603, Jun. 2012.

[2]   C. C. Jacques, J. McIntosh, S. Giovinazzi, T. D. Kirsch, T. Wilson, and J. Mitrani-Reiser, "Resilience of the Canterbury Hospital System to the 2011 Christchurch Earthquake," *Earthquake Spectra*, vol. 30, no. 1, pp. 533–554, Feb. 2014.

[3]   J. Mitrani-Reiser, C. Jacques, T. D. Kirsch, S. Giovinazzi, J. K. McIntosh, and T. M. Wilson, "Response of the Regional Health Care system to the 22nd February 2011, Christchurch Earthquake, NZ," in *Proceedings of the 15th World Conference on Earthquake Engineering*, 2012.

[4]   C. Scawthorn, "Fire following earthquake," *Fire Safety Science*, vol. 1, pp. 971–979, 1986.

[5]   T. Adachi and B. R. Ellingwood, "Serviceability of earthquake-damaged water systems: Effects of electrical power availability and power backup systems on system vulnerability," *Reliability Engineering & System Safety*, vol. 93, no. 1, pp. 78–88, Jan. 2008.

[6]   S.-R. Han, S. D. Guikema, S. M. Quiring, K.-H. Lee, D. Rosowsky, and R. A. Davidson, "Estimating the spatial distribution of power outages during hurricanes in the Gulf coast region," *Reliability Engineering & System Safety*, vol. 94, no. 2, pp. 199–210, Feb. 2009.

[7]   J. Izquierdo, I. Montalvo, R. Pérez, and M. Herrera, "Sensitivity analysis to assess the relative importance of pipes in water distribution networks," *Mathematical and Computer Modelling*, vol. 48, no. 1–2, pp. 268–278, Jul. 2008.

[8]   N. Romero, L. K. Nozick, I. Dobson, N. Xu, and D. A. Jones, "Seismic retrofit for electric power systems," *Earthquake Spectra*, vol. 31, no. 2, pp. 1157–1176, 2015.

[9]   A. M. Salman, Y. Li, and M. G. Stewart, "Evaluating system reliability and targeted hardening strategies of power distribution systems subjected to hurricanes," *Reliability Engineering & System Safety*, vol. 144, pp. 319–333, Dec. 2015.

[10]   Y. Dutuit and A. Rauzy, "On the extension of Importance Measures to complex components," *Reliability Engineering & System Safety*, vol. 142, pp. 161–168, Oct. 2015.

[11]   C. A. Davis and S. Giovinazzi, "Toward Seismic Resilient Horizontal Infrastructure Networks," 2015.

[12]   S. Esposito, I. Iervolino, A. d'Onofrio, A. Santo, F. Cavalieri, and P. Franchin, "Simulation-Based Seismic Risk Assessment of Gas Distribution Networks: Seismic risk assessment of gas networks," *Computer-Aided Civil and Infrastructure Engineering*, vol. 30, no. 7, pp. 508–523, Jul. 2015.

[13]   Caltrans, "Caltrans Seismic Design Criteria Version 1.7," California Department of Transportation, Sacramento, CA, 2013.

[14]   M. Miller, "Seismic risk assessment of complex transportation networks," Stanford University, 2014.

[15]   L. A. Rossman, *EPANET 2 Users Manual*. Cincinnati, OH: United States Environmental Protection Agency, 2000.

[16]   J. J. Bommer and H. Crowley, "The Influence of Ground-Motion Variability in Earthquake Loss Modelling," *Bulletin of Earthquake Engineering*, vol. 4, no. 3, pp. 231–248, Mar. 2006.

[17]   J. Park, P. Bazzurro, and J. Baker, "Modeling spatial correlation of ground motion intensity measures for regional seismic hazard and portfolio loss estimation," in *Tenth International Conference on Application of Statistic and Probability in Civil Engineering*, Tokyo, Japan, 2007.

[18]   H. Crowley, "Earthquake Risk Assessment: Present Shortcomings and Future Directions," in *Perspectives on European Earthquake Engineering and Seismology*, vol. 34, A. Ansal, Ed. Cham: Springer International Publishing, 2014, pp. 515–532.

[19]   E. H. Field, T. H. Jordan, and C. A. Cornell, "OpenSHA: A Developing Community-modeling Environment for Seismic Hazard Analysis," *Seismological Research Letters*, vol. 74, no. 4, pp. 406–419, Jul. 2003.

[20]   Working Group on California Earthquake Probabilities, "The Uniform California Earthquake Rupture Forecast, Version 2," U.S. Geological Survey Open-File Report 2007-1437 and California Geological Survey Special Report 203, 2008.

[21]   P. Bazzurro and N. Luco, "Effects of different sources of uncertainty and correlation on earthquake-generated losses," *Australian Journal of Civil Engineering*, vol. 4, no. 1, pp. 1–14, 2007.

[22]   N. Jayaram and J. W. Baker, "Correlation model for spatially distributed ground-motion intensities," *Earthquake Engineering & Structural Dynamics*, vol. 38, no. 15, pp. 1687–1708, Dec. 2009.

[23]   J. Wu and J. W. Baker, "Ground Motion Modeling for Risk and Reliability Assessment of San Francisco Infrastructure Systems," in *10th National Conference on Earthquake Engineering, Anchorage, Alaska, United States*, 2014.

[24]   M. Miller, "Seismic risk assessment of complex transportation networks," Stanford University, 2014.

[25]   S.-S. Jeon and T. D. O'Rourke, "Northridge Earthquake Effects on Pipelines and Residential Buildings," *Bulletin of the Seismological Society of America*, vol. 95, no. 1, pp. 294–318, Feb. 2005.

[26]   AECOM and AGS, "CS-199 Planning Support Services for Auxiliary Water Supply System (AWSS) - Technical Memorandum (TM) - Task 8 - Modeling," Jan. 2012.

[27]   American Lifelines Alliance, "Seismic Guidelines for Water Pipelines." 2005.

[28]   Federal Emergency Management Agency (FEMA), "Hazus-MH 2.1 Technical Manual." Washington D.C., 2009.

[29]   P. Shi, T. D. O'Rourke, and Multidisciplinary Center for Earthquake Engineering Research (U.S.), *Seismic response modeling of water supply systems*. Cornell University, Jan., 2006.

[30]   M. Rausand and A. Høyland, *System Reliability Theory: Models, Statistical Methods, and Applications*. John Wiley & Sons, 2004.